

Band structures of delafossite transparent conductive oxides from a self-consistent GW approachFabio Trani,^{1,2,3} Julien Vidal,^{4,5,2} Silvana Botti,^{5,1,2} and Miguel A. L. Marques^{1,2}¹*Laboratoire de Physique de la Matière Condensée et Nanostructures (LPMCN), Université Lyon 1, CNRS, Domaine Scientifique de la Doua, 69622 Villeurbanne, France*²*European Theoretical Spectroscopy Facility (ETSF)*³*Scuola Normale Superiore di Pisa, Piazza dei Cavalieri 7, 56126 Pisa, Italy*⁴*Institute for Research and Development of Photovoltaic Energy (IRDEP), UMR 7174, CNRS/EDF/ENSCP, 6 quai Watier, 78401 Chatou, France*⁵*Laboratoire des Solides Irradiés (LSI), École Polytechnique, CNRS, CEA-DSM, 91128 Palaiseau, France*

(Received 27 May 2010; revised manuscript received 7 July 2010; published 19 August 2010)

We present a comparative study of the electronic band structures of the compounds CuMO_2 ($M=\text{B, Al, In, Ga}$) which belong to the family of delafossite transparent conductive oxides. The theoretical approaches we use are the standard local-density approximation (LDA) to density-functional theory, LDA + U , hybrid functionals, and perturbative GW on top of LDA or self-consistent Coulomb hole plus screened exchange calculations. The latter approach, state-of-the-art theoretical approach for quasiparticle band structures, predicts direct band gaps that are compatible with experimental optical gaps only after including the strong polaronic and excitonic effects present in these materials. For what concerns the so-called band-gap anomaly of delafossite compounds, we find that GW approaches yield the same qualitative trends with increasing anion atomic number as the LDA: accounting for the oscillator strength at the absorption edge is the key to explain the experimental trend. None of the methods that we applied beyond the simple LDA is in agreement with the small indirect gaps found by many early experiments. This supports the recent view that the absorption bands identified as a sign of the indirect experimental gaps are likely due to defect states in the gap and are not a property of the pristine material.

DOI: [10.1103/PhysRevB.82.085115](https://doi.org/10.1103/PhysRevB.82.085115)

PACS number(s): 71.20.-b, 71.45.Gm, 78.20.-e, 71.15.Qe

I. INTRODUCTION

Transparent conductive oxides (TCOs) are wide band-gap semiconductors characterized by large free carrier densities. These carriers are created by either intrinsic or extrinsic doping, giving to TCOs both low resistivity and transparency in the visible energy window. The technological applications of these materials are wide, ranging from their use as transparent contacts in flat panel displays,¹ to photovoltaic devices.² The charge carriers are usually electrons. Indeed, the most common examples of TCOs are electron (n -)doped SnO_2 , In_2O_3 , and ZnO . Hole (p -type) conductivity in TCOs was much harder to achieve but it was ultimately found in CuAlO_2 thin films.³ A few years later, bipolar (either n - or p -type) conductivity was discovered in one element of the same family, namely, CuInO_2 .^{4,5} These spectacular achievements opened the way for the fabrication of TCO p - n junctions,⁶ and to the development of a new technology entirely based on “invisible circuits,” the so-called transparent electronics,⁷⁻⁹ with many innovative applications stemming from it, such as stacked solar cells, transparent screens, or functional windows that generate solar electricity.

The materials responsible for such amazing properties belong to a particular class of Cu ternary oxides appearing in nature in the delafossite crystal phase, CuMO_2 , where M is a group-III element.¹⁰ Their crystal structure is characterized by parallel planes composed of M and O atoms linked by dumbbell Cu atoms, yielding a strong anisotropy in the electronic properties. Since the discovery of their relatively high conductivity, delafossite copper oxides have been studied extensively both from the theoretical and the experimental

point of view, and are the object of a raising interest from the scientific community, especially for their applications in thin-film solar-cell technology.

From the experimental point of view, delafossites have been subject to conductivity and optical measurements, arguably the most important properties for their use as TCOs. The oldest optical experiments for CuAlO_2 pointed to a large difference between the direct and indirect band gap.^{3,11-18} Analogous results followed for CuInO_2 (Refs. 4, 19, and 20) and CuGaO_2 .²¹ However, the most recent experimental work²²⁻²⁴ suggests that all early results should be reanalyzed in view of the fact that most of the samples used in experiments were thin films. Indeed, the discrepancy between the gap measured for thin films and single-crystal samples hints at the fact that strain might play an important role. Moreover, one should consider that even if the extraction of the direct band gap from inspection of the absorption onset is fairly straightforward, the identification of the indirect band gap is considerably hindered by the inevitable presence of defect bands in the samples. Recent accurate single-crystal measurements²²⁻²⁴ lead to a reduction in the difference between direct and indirect band gap and an overall opening of the band gap.

From the theoretical side, Laskowski *et al.*²⁵ and Christensen *et al.*²⁶ showed that absorption at the direct edge of copper delafossites is dominated by huge excitonic effects (about 0.5 eV). Similar excitonic effects were also found in experiments for CuScO_2 .^{23,27} This fact should be always taken into account when comparing calculated quasiparticle energies and optical measurements, as the optical and quasiparticle gaps differ by the exciton binding energy. Finally, various experiments²⁸⁻³¹ point to the importance of small

polarons in the conductivity mechanism, related to a very strong electron-phonon interaction in these materials together with their layered structure. However, the most recent experiments on monocrystals²⁴ are interpreted more consistently in terms of a band conduction model with acceptors located about 700 meV above the valence band (likely Cu vacancies) supplying holes for conduction.

From the theoretical side, and in spite of many efforts, it turned out difficult for calculations to reproduce and interpret experimental measurements. Indeed, delafossite materials present a subtle hybridization of the *d* states of copper with the *p* states of oxygen close to the Fermi level. This leads to subtle exchange and correlation effects that are very hard to take into account in standard theoretical schemes. For many years the only *ab initio* method applied to delafossites was standard density-functional theory (DFT),^{5,11,21,30,32} based either on the local-density approximation (LDA) or on general gradient approximations (GGAs). However, DFT is hampered by two important shortcomings when applied in this context: (i) the Kohn-Sham band gap is systematically underestimated by 50–100 % when compared to photoemission experiments; (ii) the deficient cancellation of the spurious self-interaction terms in standard functionals, particularly critical for *d* electrons that usually are located too high in energy. For systems with shallow *d* states, such as the delafossite systems, that has a direct effect on the band gap.

In the last years, we witnessed the emergence of several techniques going beyond standard DFT, such as LDA+*U* or hybrid functionals. Both methods have been used to study elements of the delafossite family with some success.^{25,33,34} Hybrid calculations can partially fix the self-interaction problem and have proved to improve the treatment of localized states and better reproduce the band gap,³⁵ especially for materials with small and intermediate band gaps.^{36,37} They represent a major step forward with respect to LDA and GGA calculations but they should be used with care as their accuracy and reliability depends on the material under study.^{36,38} LDA+*U*³⁹ was originally designed to correct the position of the *d* states through the introduction of the on-site interaction *U*. Unfortunately, this method is not self-interaction free. Furthermore, most applications of LDA+*U* use an empirical value for *U*, which makes the method semi-empirical.

In the past years, *GW* approaches,⁴⁰ based on many-body perturbation theory, have proved to be an invaluable tool to compute accurate band gaps for a wide range of materials.^{41–43} The *GW* method solves many of the deficiencies of the previously mentioned approaches at the cost of much more involved computations. It turns out, however, that the standard, perturbative, *GW* treatment is unable to describe the band-gap physics of many transition metal oxides and sulfides, yielding too small band gaps.^{44–46} In this case, more sophisticated calculations have to be performed to obtain reliable results. To this aim, some self-consistent schemes that use approximated *GW* self-energies were proposed to allow to iteratively upgrade the quasiparticle energies and wave functions, leading to a remarkable improvement of the results.^{42–47} We have recently applied one of these methods to the study of delafossite CuAlO₂ and

CuInO₂,³⁴ providing a consistent description of the electronic states, and obtaining results that support the most recent experimental reports in the literature.^{22–24} Recently, Christensen *et al.* obtained comparable calculations for CuAlO₂ under pressure using another restricted self-consistent *GW* scheme.²⁶

Finally, we should note that most experiments rely on optical absorption or transmission, with measurements of the *optical* band gap. This is the lowest energy we need to furnish to the system to create an electron-hole pair, and includes the electron-hole (excitonic) contribution. In contrast, the *quasiparticle* band gap is defined as the energy required to promote an electron from the top valence band to the bottom conduction band. This value can be obtained through photoemission experiments, and is the one usually calculated by theory.⁴⁸ Unfortunately, there is only one photoemission measurement for the delafossite structures,¹¹ and one excitonic calculation in literature, based on the solution of the Bethe-Salpeter equation on top of a GGA+*U* band structure.²⁵ In this theoretical work it was shown that the electron-hole binding energy of CuAlO₂ is about 0.5 eV (Ref. 25) and that the first excitonic peak position is almost independent of the specific material (CuAlO₂, CuInO₂, and CuGaO₂), in contrast with the 0.4 eV energy range that separates the experimental absorption thresholds. Still, we can retain with a certain confidence that the excitonic binding energies can be as large as 0.5 eV when comparing our calculations to experiment.

In this paper, we present benchmark *GW* calculations for four members of the delafossite family, namely, CuAlO₂, CuInO₂, CuGaO₂, and CuBO₂. These calculations are also compared to standard DFT, LDA+*U*, and hybrid functional calculations. The rest of this paper is organized as follows. In Sec. II, we present the *GW* method and its different flavors. We then describe several technical issues relevant for our calculations, focusing, in particular, on the convergence with the number of unoccupied states. In Sec. III, we discuss in detail CuAlO₂, comparing different methods. We also stress the importance of polaronic effects in order to obtain results in close agreement with experimental data. In Sec. IV, we present our calculations for other members of the delafossite family (CuInO₂, CuGaO₂, and CuBO₂), and extract trends with the anion atomic number. Finally, we draw our conclusions in Sec. V.

II. METHODOLOGY

A. *GW* approaches

In 1965, Hedin⁴⁰ established a set of equations that reformulated traditional many-body theory in terms of a physically motivated *screened* interaction *W*. This set should be solved self-consistently, a task still way beyond current theoretical and computational resources. The *GW* method used for real systems is an approximation to this set of five equations, where the self-energy of the system is written as

$$\Sigma(1,2) = iG(1,2)W(1^+,2) \quad (1)$$

where *G*(1,2) is the one-particle Green's function of the system and *W*(1⁺,2) the dynamical screened Coulomb interac-

tion. The argument 1 stands for (r_1, t_1) and 1^+ means that the limit $t_1 + \eta \rightarrow t_1$ should be taken for η positive. Both G and W are themselves solutions of Dyson equations, i.e., they should be evaluated using quasiparticle wave functions and energies. Until recently, however, in most practical implementations this costly procedure has been approximated by calculating the quasiparticle energies ϵ_i^{QP} as a first-order perturbation to the Kohn-Sham eigenvalues ϵ_i^{KS} (usually obtained within LDA or GGA),

$$\epsilon_i^{\text{QP}} = \epsilon_i^{\text{KS}} + Z \langle \phi_i^{\text{KS}} | \Sigma(\epsilon_i^{\text{KS}}) - v_{\text{xc}} | \phi_i^{\text{KS}} \rangle, \quad (2)$$

where ϕ_i^{KS} are the Kohn-Sham wave functions, v_{xc} the exchange-correlation potential, and Z is the quasiparticle renormalization factor given by

$$Z = \left\{ 1 - \langle \phi_i^{\text{KS}} | \frac{\partial \Sigma(\epsilon)}{\partial \epsilon} \Big|_{\epsilon = \epsilon_i^{\text{KS}}} | \phi_i^{\text{KS}} \rangle \right\}^{-1}. \quad (3)$$

Clearly, the so-called G_0W_0 approximation of Eq. (2), or perturbative GW , is only valid when the reference Kohn-Sham energy levels and wave functions are reasonably good approximations to the quasiparticle ones. This is often the case, and indeed the G_0W_0 method provides a systematic improvement to Kohn-Sham band structure and has been extremely successful in the treatment of sp semiconductors.⁴¹ Unfortunately, this perturbative treatment turns out to be insufficient for transition metal oxides, and for materials where the bands close to the Fermi level have a significant d (or f) character, as it is the case for delafossite TCOs.

Different strategies were put forward in order to overcome this problem: (i) the choice of a better reference system, replacing the standard LDA or GGA by, e.g., exact exchange,⁴⁹ LDA+ U ,⁵⁰ or hybrid functionals.⁵¹ (ii) Using an approximate self-consistent GW scheme,^{42,47,52} in which the wave functions and eigenenergies are updated iteratively. This latter method has the great advantage of yielding results independent of the initial guess of the wave functions.

Unfortunately, the straightforward iteration of the Dyson equations in Hedin's GW framework leads to non-Hermitian self-energies that complicate considerably the scheme. Besides, it was proved that a full self-consistent procedure deteriorates the quality of the spectroscopic properties we are interested in.⁵³ Therefore, the original self-consistent GW scheme of Faleev *et al.*,⁵² that in the following we refer to as the quasiparticle self-consistent GW method (QPsc GW), relies on a Hermitianization of the self-energy. It turns out that this scheme leads to very accurate quasiparticle wave functions and energies for a large number of systems. In this paper, we chose an alternative approach to QPsc GW , that is considerably lighter from a computational point of view.^{44,47} Such approach, that we will refer to as G_0W_0 @scCOHSEX, consists in performing a self-consistent Coulomb hole plus screened exchange (COHSEX) calculation, followed by a perturbative GW on top of it. The COHSEX approximation⁵⁴ is an alternative way, proposed by Hedin in the 1960s, to approximate the GW self-energy making it Hermitian and static. In contrast with the approximation of Faleev *et al.*, it neglects completely dynamical effects, but it has the advantage that it only requires the knowledge of the occupied

manifold, which decreases considerably the computational burden.

Self-consistent COHSEX usually leads to band gaps that are too large when compared with experiment, due to the complete neglecting of dynamical effects in the screening. However, the quasiparticle wave functions turn out to be very close to the QPsc GW ones.⁴⁷ The final step of our method, the perturbative GW performed on top of the self-consistent COHSEX wave functions, accounts for the dynamical screening that was missing in the COHSEX approximation. This correction decreases the value of the gap, yielding quasiparticle energies in excellent agreement both with experiments and QPsc GW calculations.⁴⁴⁻⁴⁷

B. Numerical details

The set of methods used in this paper includes DFT in the standard LDA, LDA+ U , hybrid functionals, and GW approaches. For the hybrid functional calculations, we used the functionals HSE03 (Ref. 55) and PBE0 (Ref. 56) as implemented in VASP.^{57,58} LDA+ U and GW calculations were performed using ABINIT.⁵⁹ The value we used for U is the same empirical value used by Laskowski *et al.*,²⁵ i.e., 8 eV, in order to be able to compare directly with their results. Hybrid functionals and LDA+ U calculations were based on a PAW formalism, with a cutoff of 44 hartree for the plane wave basis. On the other hand, GW calculations were carried out using norm-conserving pseudopotentials. The Cu pseudopotential is built including $3s$ and $3p$ semicore states in the valence. Also In $4s$, $4p$, and $4d$ semicore states are taken in the valence while we verified that Ga $3d$, $3p$, and $3s$ states could be safely kept in the core. We remind that the proper treatment of semicore orbitals is crucial in GW calculations of Cu compounds.⁴⁴ A $4 \times 4 \times 4$ \mathbf{k} -point grid and an energy cutoff of 120 hartree were used for the ground-state calculations while a 90 hartree energy cutoff was used for the computation of the screening and the self-energy. The dynamical behavior of the screening in the G_0W_0 calculation was taken into account by a plasmon-pole model.⁶⁰ As the experimental and LDA-relaxed geometries are very close (within 1%), and the small contraction of the lattice in LDA has a negligible effect on band structures (corrections amount to less than 0.05 eV), we used experimental lattice parameters for CuAlO₂, CuInO₂, and CuGaO₂. In the case of CuBO₂, we performed calculations at both experimental and LDA-optimized parameters as they surprisingly differ by more than 10%. We will discuss this issue in Sec. IV C.

One of the most serious bottlenecks in GW calculations concerns the convergence with respect to the number of unoccupied bands. Indeed, both the calculation of the Green's function G and of the screened interaction W involves infinite sums over unoccupied states. It is possible to circumvent this sum, as it was recently proposed in Ref. 61 but most of the current implementations simply cutoff the infinite sum at a certain energy. Unfortunately, convergence with respect to the number of unoccupied states is often very slow, and this is indeed the case for the delafossite systems where a fully converged calculation would require thousands of empty bands (see Fig. 1). Fortunately, this situation can be dramati-

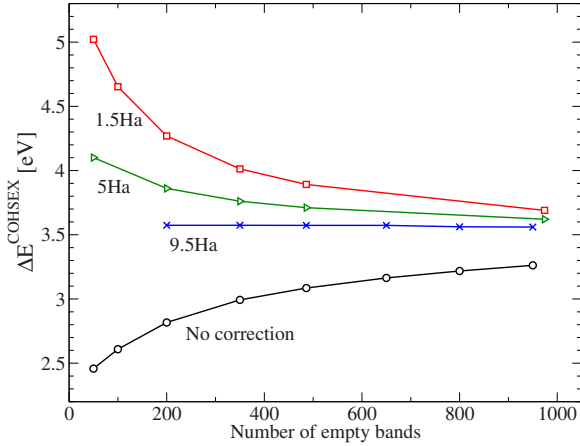


FIG. 1. (Color online) Convergence of the GW correction to the quasiparticle energies (within the COHSEX approximation) at a random \mathbf{k} point with respect to the number of unoccupied bands for CuInO_2 . Calculations performed using the method of Ref. 62, for $\epsilon=1.5$ hartree (red squares), 5 hartree (green triangles), and 9.5 hartree (blue crosses) are compared with results obtained without using it (black circles).

cally improved using the recipe of Bruneval and Gonze,⁶² where the energies of all the states that are not taken into account explicitly in the summation are replaced by a single number ϵ . This number is to some extent arbitrary, and should be chosen in order to speed up the convergence. An example, for CuInO_2 , is shown in Fig. 1 where the value of the GW correction to the LDA eigenenergies (within the COHSEX approximation) is plotted as a function of the number of unoccupied states for different values of ϵ . It is clear that for a carefully chosen ϵ , in this case of around 9.5 hartree, convergence can be reached by as few as 200 empty bands (the value used in this paper).

III. AL COMPOUND

Since p -type conductivity was first discovered in CuAlO_2 thin films,³ this compound has been extensively studied in the literature.^{5,11,13,15,18,22,25,26,32,33,63–68} However, experiments are afflicted by a large dispersion of data. Experi-

mental studies agree to indicate that CuAlO_2 is an indirect band-gap material. Different authors evaluated the indirect gap by optical measurements on thin-film samples in the range 1.65–2.1 eV. More recently, experiments on monocrystals seem to agree that a better estimate for the indirect gap is of about 3.00 eV (Refs. 22–24) while the absorption bands at lower energy are most likely assigned to impurity levels in the gap.^{22,33} Most of the measurements locate the direct gap in the range 3.4–3.7 eV. There is only one photoemission experiment¹¹ which shows that the quasiparticle band gap is comparable to the direct gap (3.5 eV). It is not clear why there is such a large discrepancy between the indirect band gap evaluated by optical transmission and the one determined by photoemission spectroscopy. There is no trace of the indirect band gap at about 2 eV in all the theoretical calculations made on the pure crystal, apart from the results coming from LDA/GGA, that, as is well known (and shown below), always underestimate the band gaps. This is a controversial point that our calculations can help to clarify.

A. GW band structures

The left panel of Fig. 2 shows the CuAlO_2 band structure, calculated using the LDA, G_0W_0 , and $G_0W_0@scCOHSEX$. Here and in the following, we use the path in the Brillouin zone suggested by Ref. 5. This path has the advantage of including the top of the valence band, that lies close to F according to all the methods we considered. Concerning the conduction band, there is a competition between two minima, at Γ and L . Within the LDA, the bottom of the conduction band lies at Γ , the minimum at L being 0.6 eV higher. However, these differences, as well as the band dispersions, depend strongly on the method employed.

First, we observe that the quasiparticle corrections calculated perturbatively within G_0W_0 are very important, leading to a \mathbf{k} -dependent opening of the band gap of up to 3.0 eV, and significantly reducing the difference between direct and indirect band gap to 0.3 eV. The absolute value of the direct band gap is in relatively good agreement with experiments, however several facts make us believe that a perturbative scheme is insufficient to describe the physics of these compounds.

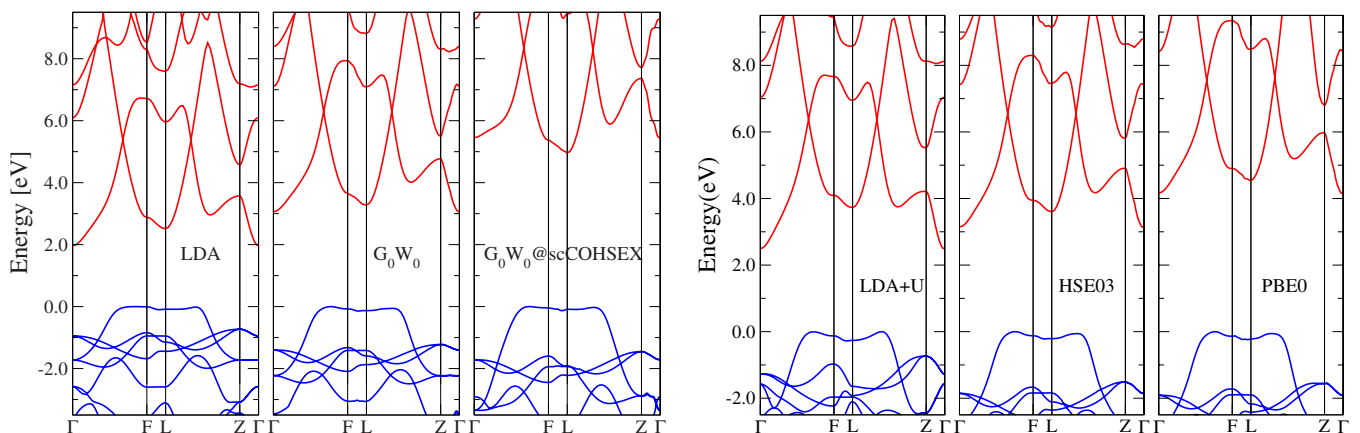


FIG. 2. (Color online) Band structures of CuAlO_2 calculated using the LDA, G_0W_0 , $G_0W_0@scCOHSEX$, LDA+ U , HSE03, and PBE0.

TABLE I. Indirect and direct band gaps of CuAlO_2 calculated with several techniques. All the energies are in electron volt. The indirect band gap is measured between the valence-band maximum close to F and the conduction-band minimum at Γ , except for the case of G_0W_0 @scCOHSEX calculations as the conduction-band minimum is located at L .

	E_{ind}	E_{dir}	$E_{\text{dir}} - E_{\text{ind}}$
Expt. ^a	1.7–3.0	2.9–3.9	0.5–2.0
LDA	2.0	2.6	0.6
G_0W_0	3.1	3.4	0.3
G_0W_0 @scCOHSEX	5.0	5.1	0.1
G_0W_0 @scCOHSEX (E only)	5.3	6.2	0.9
G_0W_0 @scCOHSEX+P	3.8	3.9	0.1
LDA+ U	2.5	4.0	1.5
HSE03	3.1	3.8	0.7
HSE06	3.6	4.1	0.5
PBE0	4.2	4.8	0.6
B3LYP (Ref. 33)	3.9	4.5	0.6

^aSee the text for the references.

Perhaps the simplest copper oxide structure where copper retains the same oxidation state Cu^+ as in the delafossites is Cu_2O . This is a p -type semiconductor characterized by a direct band gap of 2.17 eV. From Refs. 44 and 69, we learn that the DFT-LDA gap of Cu_2O is 0.54 eV. A perturbative G_0W_0 calculation opens up the gap to 1.34 eV, and only by applying the same G_0W_0 @scCOHSEX scheme that we used for this work it is possible to obtain a gap of 1.97 eV, only 10% smaller than the experimental value. It is true that the analysis of the top valence band shows that in Cu_2O the hybridization between Cu $3d$ and O $2p$ is more important (68% of Cu $3d$ and 20% of O $2p$) than in CuAlO_2 , where the valence-band maximum is almost exclusively formed by Cu $3d$ together with a small amount of O $2p$ states ($\sim 90\%$ Cu $3d$ and $\sim 10\%$ O $2p$).³⁰ However, previous GW calculations on vanadium oxide, another oxide material with a band-gap made of states with a strong $3d$ character, indicate that DFT wave functions are insufficiently localized and too symmetric.⁴⁵ All these observations point to the need of performing some kind of self-consistent GW calculations for Cu delafossites, in order to move away from the inaccurate LDA starting point. We chose to perform G_0W_0 @scCOHSEX calculations as this method yields excellent results for similar materials.^{44,46}

Our G_0W_0 @scCOHSEX results for CuAlO_2 are summarized in the left panel of Fig. 2 and Table I. The quasiparticle corrections to the LDA energies are strongly dependent on the \mathbf{k} point. The difference between indirect and direct gap decreases with the increasing complexity of the method used: G_0W_0 @scCOHSEX calculations yield an almost direct gap of 5 eV. This result is confirmed by the QPsc GW calculations of Ref. 26, although their QPsc GW gaps are slightly smaller.

It is worth noting that, by increasing the complexity level of the calculation, there is an upward shift of the conduction valley at Γ , with respect to the one at L . This fact has also

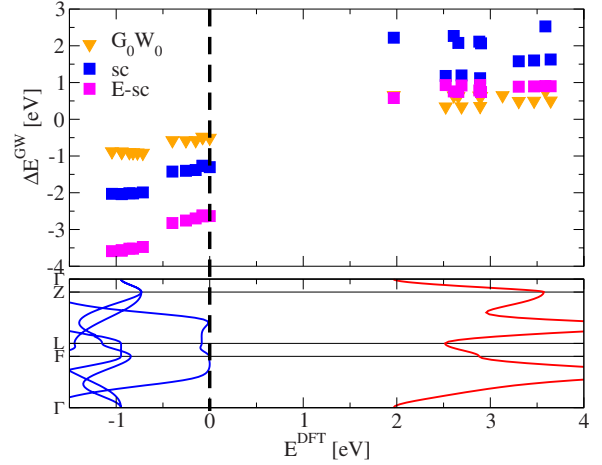


FIG. 3. (Color online) Top panel: G_0W_0 and G_0W_0 @scCOHSEX corrections to the DFT-LDA Kohn-Sham energies versus the Kohn-Sham energies for CuAlO_2 . Bottom panel: band structure of CuAlO_2 calculated in DFT-LDA.

clear implications on the selection rules for optical matrix elements (dipole transitions are forbidden at Γ , while they are allowed at L and F) and the character of the transitions that determine the features in the optical spectra of these materials.⁵

In Fig. 3, we show the quasiparticle correction to the Kohn-Sham LDA bands using G_0W_0 and G_0W_0 @scCOHSEX. For what concerns the modification of the band dispersions, the effect already seen in G_0W_0 is enhanced in G_0W_0 @scCOHSEX. Furthermore, the corrections depend strongly on the character of the band. The dramatic failure of G_0W_0 can be imputed not only to the wrong screening properties inherited from the underestimated DFT band gap (as in Cu_2O) but also to the incorrect localization properties of the DFT wave functions. To investigate further this point, we performed a G_0W_0 @scCOHSEX calculation keeping the wave functions fixed while updating iteratively only the energies (points labeled E-sc in Fig. 3 and G_0W_0 @scCOHSEX (E only) in Table I). It is clear that the self-consistency in the energies is not equivalent to the self-consistency both in the energies and the wave functions, which indicates that the wave functions are indeed strongly modified during the scCOHSEX cycles.

Moreover, the large difference between perturbative and self-consistent results shows that the LDA wave functions and energies constitute a very poor approximation to quasiparticle states in Cu delafossite materials. In addition, the fact that the GW corrections are strongly \mathbf{k} -point dependent prevent us from using a scissor operator to simulate them. We remind that the use of scissor operators on top of LDA band structures is very common in literature, often without verifying if such a drastic approximation is justified.

B. GW corrections to the valence states

Calculations performed using G_0W_0 @scCOHSEX predict an overall downshift of the highest valence states. This shift is strongly \mathbf{k} dependent. By inspection of Fig. 4 (left panel),

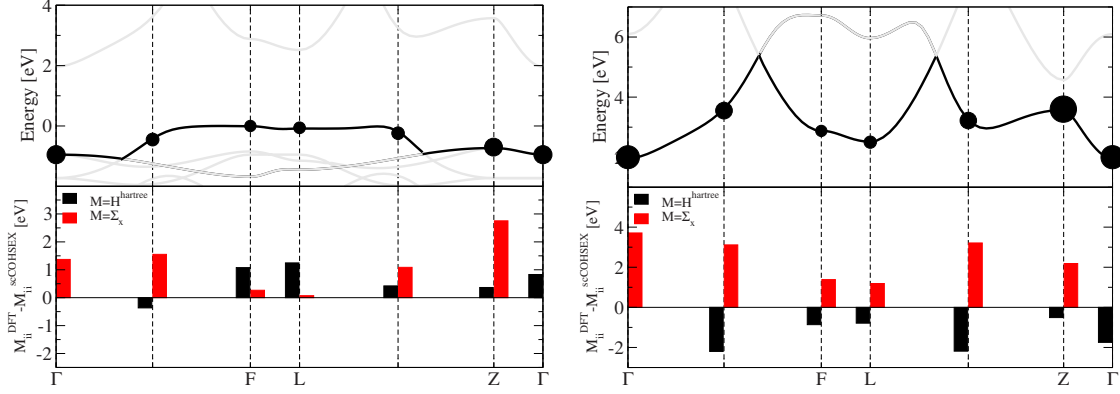


FIG. 4. (Color online) Top panels: Kohn-Sham band structure of CuAlO_2 . The size of the dots is proportional to the absolute value of the $G_0W_0@scCOHSEX$ corrections. Bottom panels: difference between the expectation value of the operator M ($M=H^{\text{Hartree}}, \Sigma_x$) constructed with DFT wave functions or with scCOHSEX wave functions for the top valence band (left panel) and for the bottom valence band (right panel).

we can conclude that this behavior is caused by strong modifications at different \mathbf{k} points of the matrix elements $\langle v|\Sigma_x|v\rangle$ and $\langle v|H^{\text{Hartree}}|v\rangle$, where the state $|v\rangle$ belongs to the top valence. This behavior can be explained by considering the different character of the top valence band in different parts of the Brillouin zone. Indeed, it is evident that there is a band crossing along the path between F and Γ , which leads to a change in character of the highest valence band (black line in the left panel of Fig. 4). Crystal-field theory predicts the splitting of the d states which contribute to the top valence in two groups, one with e_g and the other with t_{2g} symmetry. The symmetry analysis of the states coming from our calculations shows that, on the plateau which includes the F point and L point, the top valence band is mainly formed by e_g states with a small contribution of O $2p$ states. On the other hand, in the remaining part of the Brillouin Zone, the top valence band is formed by a mixture of t_{2g} states with a significant fraction of O $2p$ states.

The left panel of Fig. 4 shows the difference between $\langle i|H^{\text{Hartree}}|i\rangle$ built either using DFT or quasiparticle wave functions for the top valence states (black histograms). The same information is also plotted for the matrix element $\langle i|\Sigma_x|i\rangle$ (red histograms). For Cu_2O , these differences were rather small (<0.1 eV),⁶⁹ moreover the changes in these two terms tended to cancel one another. The situation is quite different for CuAlO_2 , and the other copper-based delafosites, where large differences add up giving rise to a strong dispersion of the quasiparticle corrections.

Already at the G_0W_0 level, the matrix elements of $\langle v|\Sigma_x|v\rangle$ and $\langle v|H^{\text{Hartree}}|v\rangle$ depend strongly on the \mathbf{k} point. Consequently, the G_0W_0 corrections show a non-negligible dispersion, as it is shown in Fig. 3. When one performs self-consistency in the COHSEX framework, updating only the eigenenergies without changing the wave functions, the corrections of the different iterations add up and lead to a large nonconstant downshift of the top valence states (see again Fig. 3). A self-consistent procedure that includes also the update of the wave functions decreases the final correction and its dispersion, due to compensating effects coming from the changes in the wave functions. However, the G_0W_0 and $G_0W_0@scCOHSEX$ correction to the top valence bands keep differing by more than 1 eV.

For valence states with a large e_g character, the Hartree term changes significantly. This can be explained by the fact that the states are mainly of d_{z^2} character and are oriented along the bond Cu-O, overlapping considerably with the bonding density. For the bands with t_{2g} character, the main change is in the expectation value of the Fock operator. From this results it is clear that, in cases where one is interested in the band-edge correction—like for calculation of the formation energy of defects⁷⁰ or band offsets⁷¹—the use of a self-consistent scheme where also the wave functions are updated is essential.

C. GW corrections to the conduction states

To a large extent the situation for the conduction states is analogous to the one for the valence. Also in this case, there is a crossing of the lowest conduction bands yielding a change in character: close to the high-symmetry points L and F the bottom conduction states are mainly composed of Cu and O s and p orbitals; around Z and Γ the band has a Cu $3d$ character (e_g symmetry), with a significant amount of s and p states from Al, O, and Cu.

Not surprisingly, the lowest empty band has G_0W_0 corrections whose size at each \mathbf{k} is correlated with the character of the state: as a result, the corrections display a remarkable \mathbf{k} dependence, which is shown in Fig. 3. Once again, the self-consistency in the wave functions plays a considerable role. However, this time it increases the total correction with respect to the calculation where only eigenenergies are updated. The right panel of Fig. 4 shows the expectation values of the exchange self-energy $\langle c|\Sigma_x|c\rangle$ and the Hartree potential $\langle c|H^{\text{Hartree}}|c\rangle$, where $|c\rangle$ is a bottom conduction state, calculated using either DFT or scCOHSEX wave functions. For the \mathbf{k} points where the lowest conduction band has mainly s and p character, the changes in the expectation values are small and have opposite signs. This is in agreement with the fact that G_0W_0 is usually a good approximation for sp semiconductors. However, for \mathbf{k} points where the lowest conduction band has mainly a d_{z^2} character, the expectation value of the exchange operator changes considerably with the change in the wave functions. This is the driving mechanism

for the switch from indirect to quasidirect band gap in CuAlO_2 .

D. LDA+ U and hybrid functionals

The right panel of Fig. 2 shows the band structures obtained using LDA+ U and hybrid functionals (HSE03 and PBE0). The LDA+ U results, in good agreement with the previously published GGA+ U results of Ref. 25, are the only ones that show a larger upward shift of the conduction valley at L than the one at Γ . As a consequence, LDA+ U yields even a larger difference between the direct and indirect band gap than LDA (1.5 eV—see Table I), very close to the largest values obtained in early experiments. Note that all other approaches yield much smaller differences between the direct and indirect band gap, and indirect band gaps much larger than the experimental values for thin films. In view of that, such agreement is likely to be fortuitous since it is not supported either by any other theoretical method or by the most recent experiments for single crystals.²²

Concerning the hybrid functional calculations, Fig. 2 shows a great similarity between the band structures calculated using HSE03 and PBE0 functionals. Valence bands are almost identical, and very similar to the ones calculated using $G_0W_0@scCOHSEX$. Concerning the conduction bands, PBE0 results differ from HSE03 by a nearly rigid shift, and are very close to $G_0W_0@scCOHSEX$ results. This is not surprising as the PBE0 functional is particularly adequate to study materials with gaps larger than 3 eV (Ref. 72) while the quality of HSE03 gaps is known to start deteriorating in that same energy range.³⁶

By comparing the theoretical band structures with experiments, the unexpected result is the disagreement between the experimental and $G_0W_0@scCOHSEX$ direct gap (see Table I). Even taking into account a large electron-hole binding energy (of about 0.5 eV), the $G_0W_0@scCOHSEX$ band gap is more than 1 eV larger than optical measurements. The explanation of this disagreement lies in the extremely strong electron-phonon interaction present in the delafossite compounds,³⁴ as it is conveyed by the large polaron constant⁶⁴ $\alpha_p \sim 1$ for CuAlO_2 , which is the sign of a large polaronic contribution to the band gap.

Unfortunately, a fully *ab initio* many body calculation that includes electron-electron interactions together with polaronic terms is currently out of reach. Nevertheless, it is possible to include polaronic effects in a GW calculation by using a model recently proposed in Ref. 73, that relies on the knowledge of the electronic and lattice contributions to the static dielectric functions. This model consists in modifying the dielectric constant entering in the self-energy calculation to match the measured static dielectric constant⁶⁴ (that obviously includes polaronic effects). In our framework, this is only performed in the perturbative GW step, after having determined the $scCOHSEX$ wave functions to be used as better starting point for the last perturbative step. This approach, that we refer to as $G_0W_0@scCOHSEX+P$, leads to a rigid shift downward of the CuAlO_2 conduction bands by 1.2 eV (see Table I). This value is perfectly in line with what can be expected for ionic compounds characterized by such a

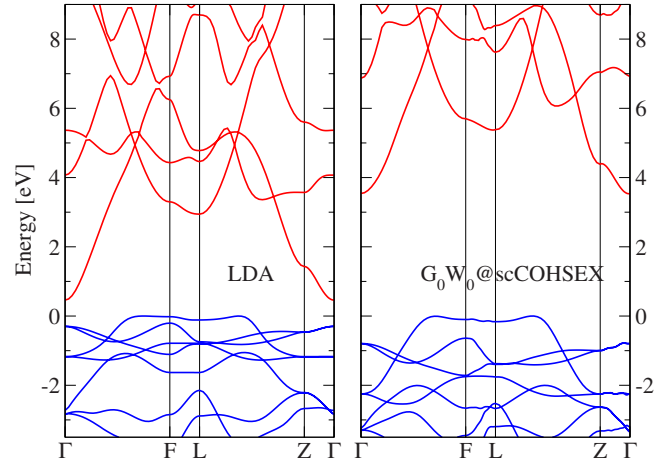


FIG. 5. (Color online) Band structure of CuInO_2 calculated using LDA and $scGW$.

large polaronic constant.⁷³ The direct band gap resulting from the $G_0W_0@scCOHSEX+P$ approach is finally 3.9 eV. The value agrees very well with the experimental optical band gaps, especially when an excitonic contribution of about 0.5 eV is also considered. We remark that we expect a negligible polaronic correction to the latter quantity, as in the case of such a strongly bound exciton the lattice cannot follow the formation of electron-hole pairs and the Coulomb attraction which enters in the excitonic Hamiltonian is to a very good approximation only screened by the redistribution of electrons.⁷³

IV. OTHER DELAFOSSITE TRANSPARENT CONDUCTIVE OXIDES

A. CuInO_2

Soon after the discovery of p -type conductivity in CuAlO_2 ,¹¹ the same research group found bipolar conductivity in CuInO_2 thin films.⁴ According to the type of doping, CuInO_2 thin films can show either n - or p -type conductivity. This led to the fabrication of p - n homojunctions,⁶ giving a boost to the emerging field of transparent electronics.^{7,8} According to experiments, CuInO_2 is characterized by a direct optical gap of 3.9–4.45 eV (Refs. 4, 19, and 20) and a small indirect gap of 1.44 eV, thus exhibiting a larger difference between direct and indirect band gaps⁵ than CuAlO_2 . Another peculiar feature is that the fundamental direct band gap lies at Γ , and is optically forbidden by symmetry reasons. A comparison to spectroscopic measurements thus requires a more detailed study, that focuses on the first allowed transitions at L and not on the fundamental direct band gap at Γ . For this reason, in the following we present direct band gaps at L .

Figure 5 shows the LDA and $G_0W_0@scCOHSEX$ band structures calculated for CuInO_2 . As already seen for CuAlO_2 , $G_0W_0@scCOHSEX$ leads to a huge opening of the band gaps: the direct band gap at L is 5.54 eV whereas the fundamental indirect gap has an energy of 3.54 eV. Furthermore, the $G_0W_0@scCOHSEX$ correction is quite sensitive to the \mathbf{k} point. With respect to the LDA, the

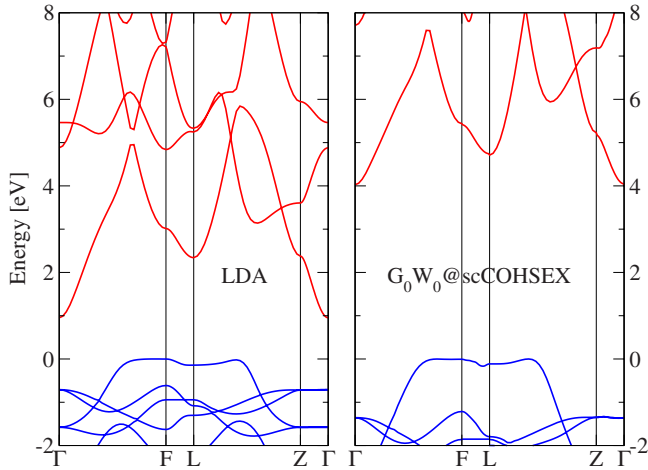


FIG. 6. (Color online) CuGaO_2 band structure calculated using LDA and scGW .

$G_0W_0@scCOHSEX$ approach leads to a decrease in the difference between direct and indirect gap, going from 2.6 eV (LDA) to 2 eV ($G_0W_0@scCOHSEX$). Just like in the case of CuAlO_2 , the present calculations locate the indirect band gap of CuInO_2 at much higher energies when compared to experiment. Once more, our results support the idea that the presence of impurity states within the forbidden gap might be responsible for the experimentally detected low-energy features.^{22,33}

The quasiparticle direct band gap at L differs by 1.6 eV from the optical band gap reported in optical/transmission measurements. This difference is comparable to what we found for CuAlO_2 , making us believe that also in this compound the excitonic and polaronic effects can be at the origin of the overestimation of the band gap by $G_0W_0@scCOHSEX$. Unfortunately, the lack of precise measurements of the static dielectric constants of CuInO_2 did not allow us to perform a model calculation of the polaronic contribution for this material. Our preliminary calculations suggest that also the exciton binding energy of CuInO_2 is about 0.5 eV, in agreement with results of Ref. 25.

B. CuGaO_2

Another interesting compound belonging to the Cu delafossite family is CuGaO_2 .²¹ Figure 6 shows the band structure of CuGaO_2 calculated using LDA and $G_0W_0@scCOHSEX$. This material has an electronic structure intermediate between CuAlO_2 and CuInO_2 , with the bottom of the conduction band at Γ and the valence-band maximum close to F. Also in this case, $G_0W_0@scCOHSEX$ calculations lead to a shrinkage of the conduction band width, and a widening of the valence band width with respect to the LDA calculations. Moreover, as it happens for CuAlO_2 and CuInO_2 , the change in dispersion of the lowest conduction band due to GW corrections increases the gap at Γ by a larger amount than the gap at L. In the case of CuInO_2 since the LDA gap at Γ was much smaller than the gap at L, the order of the direct gaps was not changed. In CuGaO_2 , instead, the GW corrections make the direct gap at L smaller

than the one at Γ . Within $G_0W_0@scCOHSEX$, the indirect and direct (at L) band gaps are 4.03 eV and 4.83 eV, respectively. The difference between the direct and indirect gap is 0.8 eV. This value is smaller than in CuInO_2 and larger than in CuAlO_2 . The direct gap can be compared to transmission spectra measurements which report an optical band gap of 3.6 eV.²¹ The discrepancy between the theoretical quasiparticle gap and the experimental optical gap is of 1.2 eV. This result is compatible with what we found for the other two compounds considered so far.

C. CuBO_2

Recently, Snure and Tiwari⁷⁴ reported the fabrication and characterization of CuBO_2 thin films. This new material appeared technologically attractive as it presents a relatively large p -type conductivity, higher than for CuAlO_2 thin films. Moreover, the authors found that the CuBO_2 optical band gap is much larger than for all other Cu delafossite compounds. However, a theoretical article by Scanlon *et al.*⁷⁵ questioned the validity of the experimental lattice parameters measured by Snure and Tiwari, as they were in disagreement by more than 10% with the theoretical values obtained using either LDA or hybrid (HSE06) functionals. This result was quite unexpected, as DFT calculations using LDA or GGA usually (and, in particular, for the other delafossite structures) give good estimations of the lattice parameters, within few percent. In view of this fact, we performed a structural optimization of CuBO_2 using the LDA, obtaining the following lattice parameters, $a=2.49$ and $c=16.34$ Å. These values should be compared with the experimental findings, $a=2.84$ and $c=16.52$ Å. In agreement with what reported in Ref. 75, this discrepancy is unusually large. Therefore, in order to shed light onto this issue and understand the effect of the geometry on the electronic band structure of CuBO_2 , we performed $G_0W_0@scCOHSEX$ calculations for the two (experimental and theoretical) configurations.

Figure 7 shows LDA and $G_0W_0@scCOHSEX$ calculations for CuBO_2 , using either the LDA-optimized (top panels) or the experimental geometry (bottom panels). With the experimental geometry, we obtained band structures similar in shape to the ones of CuGaO_2 while the LDA-optimized geometry gives bands closer to those of CuAlO_2 . Moreover, we can observe that (i) the conduction band at Γ has a significantly larger effective mass when the LDA-optimized geometry is used. (ii) The band structures at the experimental geometry have more bands in the selected energy window around the gap, as a consequence we may expect a stronger absorption at low energies than for the LDA-optimized case. (iii) The conduction-band minimum is at Γ for the experimental geometry while the LDA-optimized geometry locates that minimum at L.

Considering the series B, Al, Ga, and In, where the atoms are ordered with the increasing atomic numbers, our remarks suggest that the atomic structure of CuBO_2 given by LDA simulations gives results more in line with the trend shown by the other compounds of the family. In fact, the direct band gap calculated within $G_0W_0@scCOHSEX$ is at L and has the value of 3.52 eV. In contrast with all the other compounds,

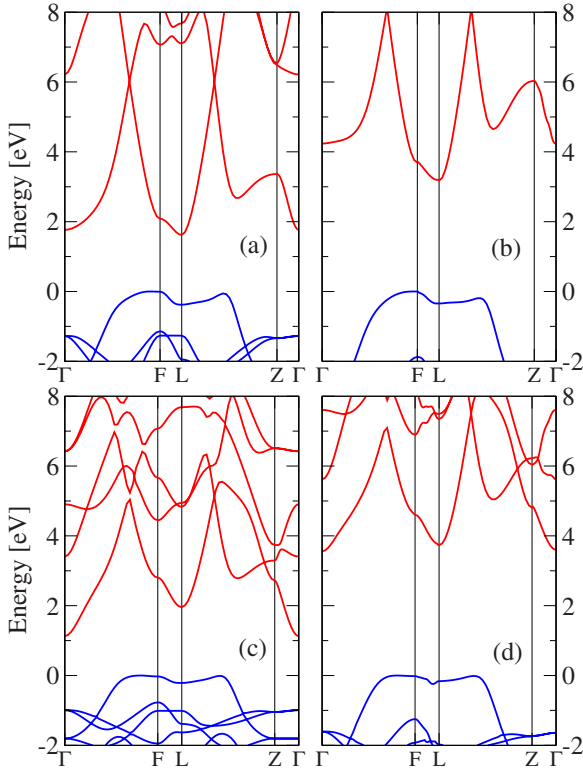


FIG. 7. (Color online) Band structures for CuBO_2 calculated using LDA [Panels (a) and (c)] and $G_0W_0@scCOHSEX$ [Panels (b) and (d)]. The top panels refer to the calculations performed using the LDA-optimized lattice parameters, the bottom panels correspond to the calculations with the experimental parameters of Ref. 74.

this value is much smaller than the reported experimental optical gap of 4.5 eV, obtained by Snure and Tiwari from transmission spectra.⁷⁴ This fact is very surprising. Snure and Tiwari measured also an indirect band gap of 2.2 eV.⁷⁴ This time the measured value is in line with the indirect gaps found for the other Cu delafossites. The $G_0W_0@scCOHSEX$ calculations yield an indirect band gap of 3.18 eV, which is considerably larger than the experimental value. It is worth stressing that the present $G_0W_0@scCOHSEX$ results are in nice agreement with the previous study of Scanlon *et al.*,⁷⁵ where calculations were performed using the hybrid functional HSE06, and where the direct and indirect band gaps were found at 3.59 eV and 3.08 eV, respectively.

D. Trends with increasing anion atomic number

We summarize the results for all the compounds we have studied in Table II, where we report the optically active direct gaps (at L), the indirect band gaps and their differences calculated within $G_0W_0@scCOHSEX$. The last column is the difference between the $G_0W_0@scCOHSEX$ and the LDA direct band gap at L. The compounds are listed in order of ascending anion atomic number.

The compounds containing Al, Ga, and In respect a clear trend. Upon increasing the anion atomic number, there is a decrease in the indirect band gap. The direct band gap, in-

TABLE II. Indirect, direct band gaps, and their differences calculated for several materials using $G_0W_0@scCOHSEX$. The last column is the $G_0W_0@scCOHSEX$ correction to the direct gap with respect to the LDA value. We show the direct gaps at L as the selection rules forbid dipole transitions at Γ . All energies are in electron volt.

	E_{ind}^{GW}	E_{dir}^{GW}	$E_{\text{dir}}^{GW} - E_{\text{ind}}^{GW}$	$E_{\text{dir}}^{GW} - E_{\text{dir}}^{\text{LDA}}$
CuBO_2^a	3.18	3.52	0.34	1.52
CuBO_2^b	3.56	3.90	0.34	1.72
CuAlO_2	4.96	5.05	0.09	2.45
CuGaO_2	4.03	4.83	0.80	2.48
CuInO_2	3.53	5.55	2.02	2.49

^aLDA-optimized lattice parameters.

^bExperimental lattice parameters, taken from Ref. 74.

stead, slightly decreases going from CuAlO_2 to CuGaO_2 , increasing afterward for CuInO_2 , in qualitative agreement with previous LDA calculations. This behavior is due to the change in dispersion of the lowest conduction band, which favors a smaller direct gap at L for the compounds containing B and Al while the direct band gaps is at Γ for the In compound. The compound with Ga has the smallest direct gap at Γ within LDA while $G_0W_0@scCOHSEX$ calculations locate the smallest direct gap at L.

The trend followed by the measured optical band gaps of CuAlO_2 , CuInO_2 and CuGaO_2 (the so-called band-gap anomaly) was studied by Nie *et al.* at the LDA level.⁵ The band-gap anomaly refers to the fact that the optical band gap increases with the increase in the anion atomic number (3.5 eV in CuAlO_2 , 3.6 eV in CuGaO_2 , and 3.9 eV in CuInO_2). Nie *et al.* concluded that it was necessary to take into account the matrix elements for optical transitions between states around the gap to reproduce the experimental order of the optical absorption edges. Our results agree qualitatively with their conclusions, even if the $G_0W_0@scCOHSEX$ results are very different from a quantitative point of view. From the last column of the table, we realize that the $G_0W_0@scCOHSEX$ corrections to the LDA band gaps are rather constant (~ 2.5 eV) for all these three compounds.

Finally, it is worth noting that the difference between the direct and indirect band gaps increases with the anion atomic number, going from 0.09 eV in CuAlO_2 (where the conduction-band minimum changes to L), to 0.8 eV in CuGaO_2 and 2.02 eV in CuInO_2 .

The situation is very puzzling for CuBO_2 . First, all band gaps are much smaller than the ones calculated for the other compounds (in contrast with experiment), particularly when one looks at the direct band gap. The difference between the direct gap and indirect gaps is 0.34 eV, and this value is independent of the geometrical structure for the two geometries we considered. The difference between $G_0W_0@scCOHSEX$ and LDA gaps is about 1.5 eV, and even in this case the dependence on the geometry is slight. This energy is much smaller than the correction of 2.5 eV reported for all the other compounds, leading us to see CuBO_2 as an atypical compound within the class of Cu delafossites.

V. CONCLUSIONS

We studied the electronic structure of Cu delafossites using a many-body perturbation technique based on a restricted self-consistent GW approach, nowadays the state of the art in band-structure calculations. In the case of CuAlO_2 , the most studied material in the literature, we applied several techniques (LDA, LDA+ U , hybrid functionals, G_0W_0 , $G_0W_0@scCOHSEX$) and compared the results with previous calculations and experimental data available in literature. We also analyzed the trend in the electronic structure of delafossites upon changing the anion atomic number, by applying the $G_0W_0@scCOHSEX$ approach to CuInO_2 , CuGaO_2 , and CuBO_2 . For the case of CuBO_2 , and in view of the surprising discrepancy between experimental and theoretical geometries, we performed calculations for both the theoretical and experimental structure.

We showed that $G_0W_0@scCOHSEX$ calculations yield band gaps much larger than the experimental data, even considering the exciton binding energy, and larger than any other *ab initio* method. This can be explained by including the polaronic contribution to the band gap. We estimated this contribution in our GW calculations using a simple model that relies on the knowledge of the electronic and lattice contributions to the static dielectric functions. Furthermore, we found that (i) both LDA and LDA+ U techniques are not able to give quantitative band structures and wave functions for delafossite compounds; (ii) the agreement often found by LDA+ U or hybrid functional calculations with experiments is somehow fortuitous, as they compensate the underestimation of the band gaps with the neglect of polaronic effects.

Furthermore, in all these compounds, experiments report an indirect band gap at very low energies, that all methods beyond the simple LDA fail to reproduce. In particular, both hybrid functionals and $G_0W_0@scCOHSEX$ calculations

yield indirect gaps at much higher energy than experimental data. This points to the fact, already suggested in literature, that impurity states located in the gap are responsible for the experimental absorption peaks that are interpreted as a signature of an indirect absorption edge.

The comparison of delafossite compounds shows that the trends among the delafossite family obtained using $G_0W_0@scCOHSEX$ are in qualitative agreement with the trends already predicted by LDA calculations. Furthermore, our calculations show that the $G_0W_0@scCOHSEX$ corrections to the direct gap are essentially independent of the compound, and that the difference between direct and indirect gaps increases with the atomic number of the anion. CuBO_2 is the exception to this rule: $G_0W_0@scCOHSEX$ correction energies are much smaller than in the other compounds, and the difference between the direct and indirect gaps does not follow the trend. We conclude that CuBO_2 is an atypical compound in this class of delafossites, that clearly needs further investigation both experimentally and theoretically.

ACKNOWLEDGMENTS

We thank Fabien Bruneval for many interesting discussions. Part of the calculations were performed at the LCA of the University of Coimbra and at IDRIS (project x2010096017). S.B. acknowledges financial support from EU Seventh Framework Programme through the e-I3 contract ETSF and the Programme PIR Matriaux-MaProSu of CNRS. M.A.L.M. acknowledges partial support from the Portuguese FCT through the Project No. PTDC/FIS/73578/2006 and from the French ANR (Grant No. ANR-08-CEXC8-008-01). J.V. acknowledges support by EDF/ANR CIFRE.

¹T. Minami, *Semicond. Sci. Technol.* **20**, S35 (2005).

²E. Fortunato, D. Ginley, H. Hosono, and D. Paine, *MRS Bull.* **32**, 242 (2007).

³H. Kawazoe, M. Yasukawa, H. Hyodo, M. Kurita, H. Yanagi, and H. Hosono, *Nature (London)* **389**, 939 (1997).

⁴H. Yanagi, T. Hase, S. Ibuki, K. Ueda, and H. Hosono, *Appl. Phys. Lett.* **78**, 1583 (2001).

⁵X. Nie, S. H. Wei, and S. B. Zhang, *Phys. Rev. Lett.* **88**, 066405 (2002).

⁶H. Yanagi, K. Ueda, H. Ohta, M. Orita, M. Hirano, and H. Hosono, *Solid State Commun.* **121**, 15 (2001).

⁷G. Thomas, *Nature (London)* **389**, 907 (1997).

⁸H. Ohta, K. Nomura, H. Hiramatsu, K. Ueda, T. Kamiya, M. Hirano, and H. Hosono, *Solid-State Electron.* **47**, 2261 (2003).

⁹A. Banerjee and K. Chattopadhyay, *Prog. Cryst. Growth Charact. Mater.* **50**, 52 (2005).

¹⁰M. N. Huda, Y. Yan, A. Walsh, S.-H. Wei, and M. M. Al-Jassim, *Phys. Rev. B* **80**, 035205 (2009).

¹¹H. Yanagi, S. Inoue, K. Ueda, H. Kawazoe, H. Hosono, and N. Hamada, *J. Appl. Phys.* **88**, 4159 (2000).

¹²C. Ong and H. Gong, *Thin Solid Films* **445**, 299 (2003).

¹³T. Dittrich, L. Dloczik, T. Guminskaya, M. Lux-Steiner, N. Grigorieva, and I. Urban, *Appl. Phys. Lett.* **85**, 742 (2004).

¹⁴E. Alkoy and P. Kelly, *Vacuum* **79**, 221 (2005).

¹⁵A. Banerjee, R. Maity, and K. Chattopadhyay, *Mater. Lett.* **58**, 10 (2004).

¹⁶A. Banerjee and K. Chattopadhyay, *J. Appl. Phys.* **97**, 084308 (2005).

¹⁷A. Banerjee, C. Ghosh, S. Das, and K. Chattopadhyay, *Physica B* **370**, 264 (2005).

¹⁸R.-S. Yu, S.-C. Liang, C.-J. Lu, D.-C. Tasi, and F.-S. Shieu, *Appl. Phys. Lett.* **90**, 191117 (2007).

¹⁹C. W. Teplin, T. Kaydanova, D. L. Young, J. D. Perkins, D. S. Ginley, A. Ode, and D. W. Readey, *Appl. Phys. Lett.* **85**, 3789 (2004).

²⁰M. Sasaki and M. Shimode, *J. Phys. Chem. Solids* **64**, 1675 (2003).

²¹K. Ueda, T. Hase, H. Yanagi, H. Kawazoe, H. Hosono, H. Ohta, M. Orita, and M. Hirano, *J. Appl. Phys.* **89**, 1790 (2001).

²²J. Pellicer-Porres, A. Segura, A. Gilliland, A. Munoz, P. Rodriguez-Hernandez, D. Kim, M. Lee, and T. Kim, *Appl.*

- Phys. Lett.* **88**, 181904 (2006).
- ²³S. Gilliland, J. Pellicer-Porres, A. Segura, A. Muñoz, P. Rodríguez-Hernández, D. Kim, M. S. Lee, and T. Y. Kim, *Phys. Status Solidi B* **244**, 309 (2007).
- ²⁴J. Tate, H. L. Ju, J. C. Moon, A. Zakutayev, A. P. Richard, J. Russell, and D. H. McIntyre, *Phys. Rev. B* **80**, 165206 (2009).
- ²⁵R. Laskowski, N. E. Christensen, P. Blaha, and B. Palanivel, *Phys. Rev. B* **79**, 165209 (2009).
- ²⁶N. E. Christensen, A. Svane, R. Laskowski, B. Palanivel, P. Modak, A. N. Chantis, M. van Schilfgaarde, and T. Kotani, *Phys. Rev. B* **81**, 045203 (2010).
- ²⁷S. Gilliland, J. Sanchez-Royo, J. Pellicer-Porres, A. Segura, A. Munoz, P. Rodriguez-Hernandez, and J. Lopez-Solano, *Thin Solid Films* **516**, 1431 (2008).
- ²⁸H. Kawazoe, H. Yanagi, K. Ueda, and H. Hosono, *MRS Bull.* **25**, 28 (2000).
- ²⁹N. Duan, A. Sleight, M. Jayaraj, and J. Tate, *Appl. Phys. Lett.* **77**, 1325 (2000).
- ³⁰B. J. Ingram, T. O. Mason, R. Asahi, K. T. Park, and A. J. Freeman, *Phys. Rev. B* **64**, 155114 (2001).
- ³¹B. Ingram, M. Bertoni, K. Poepelmeier, and T. Mason, *Thin Solid Films* **486**, 86 (2005).
- ³²B. Falabretti and J. Robertson, *J. Appl. Phys.* **102**, 123703 (2007).
- ³³J. Robertson, P. Peacock, M. Towler, and R. Needs, *Thin Solid Films* **411**, 96 (2002).
- ³⁴J. Vidal, F. Trani, F. Bruneval, M. A. L. Marques, and S. Botti, *Phys. Rev. Lett.* **104**, 136401 (2010).
- ³⁵E. N. Brothers, A. F. Izmaylov, J. O. Normand, V. Barone, and G. E. Scuseria, *J. Chem. Phys.* **129**, 011102 (2008).
- ³⁶J. Paier, M. Marsman, and G. Kresse, *Phys. Rev. B* **78**, 121201(R) (2008).
- ³⁷J. Hafner, *J. Comput. Chem.* **29**, 2044 (2008).
- ³⁸J. Paier, M. Marsman, and G. Kresse, *J. Chem. Phys.* **127**, 024103 (2007).
- ³⁹V. I. Anisimov, J. Zaanen, and O. K. Andersen, *Phys. Rev. B* **44**, 943 (1991).
- ⁴⁰L. Hedin, *Phys. Rev.* **139**, A796 (1965).
- ⁴¹W. G. Aulbur, L. Jönsson, and J. Wilkins, *Solid State Phys.* **54**, 1 (1999).
- ⁴²M. van Schilfgaarde, T. Kotani, and S. Faleev, *Phys. Rev. Lett.* **96**, 226402 (2006).
- ⁴³T. Kotani, M. van Schilfgaarde, and S. V. Faleev, *Phys. Rev. B* **76**, 165106 (2007).
- ⁴⁴F. Bruneval, N. Vast, L. Reining, M. Izquierdo, F. Sirotti, and N. Barrett, *Phys. Rev. Lett.* **97**, 267601 (2006).
- ⁴⁵M. Gatti, F. Bruneval, V. Olevano, and L. Reining, *Phys. Rev. Lett.* **99**, 266402 (2007).
- ⁴⁶J. Vidal, S. Botti, P. Olsson, J.-F. Guillemoles, and L. Reining, *Phys. Rev. Lett.* **104**, 056401 (2010).
- ⁴⁷F. Bruneval, N. Vast, and L. Reining, *Phys. Rev. B* **74**, 045102 (2006).
- ⁴⁸G. Onida, L. Reining, and A. Rubio, *Rev. Mod. Phys.* **74**, 601 (2002).
- ⁴⁹P. Rinke, A. Qteish, J. Neugebauer, C. Freysoldt, and M. Scheffler, *New J. Phys.* **7**, 126 (2005).
- ⁵⁰E. Kioupakis, P. Zhang, M. L. Cohen, and S. G. Louie, *Phys. Rev. B* **77**, 155114 (2008).
- ⁵¹F. Fuchs, J. Furthmüller, F. Bechstedt, M. Shishkin, and G. Kresse, *Phys. Rev. B* **76**, 115109 (2007).
- ⁵²S. V. Faleev, M. van Schilfgaarde, and T. Kotani, *Phys. Rev. Lett.* **93**, 126406 (2004).
- ⁵³B. Holm and U. von Barth, *Phys. Rev. B* **57**, 2108 (1998).
- ⁵⁴L. Hedin and S. Lundqvist, *Solid State Phys.* **23**, 1 (1970).
- ⁵⁵J. Heyd, G. Scuseria, and M. Ernzerhof, *J. Chem. Phys.* **118**, 8207 (2003).
- ⁵⁶C. Adamo and V. Barone, *J. Chem. Phys.* **110**, 6158 (1999).
- ⁵⁷G. Kresse and J. Furthmüller, *Comput. Mater. Sci.* **6**, 15 (1996).
- ⁵⁸G. Kresse and J. Furthmüller, *Phys. Rev. B* **54**, 11169 (1996).
- ⁵⁹X. Gonze *et al.*, *Z. Kristallogr.* **220**, 558 (2005).
- ⁶⁰R. W. Godby and R. J. Needs, *Phys. Rev. Lett.* **62**, 1169 (1989).
- ⁶¹P. Umari, G. Stenuit, and S. Baroni, *Phys. Rev. B* **79**, 201104(R) (2009).
- ⁶²F. Bruneval and X. Gonze, *Phys. Rev. B* **78**, 085125 (2008).
- ⁶³A. Banerjee, S. Kundoo, and K. Chattopadhyay, *Thin Solid Films* **440**, 5 (2003).
- ⁶⁴J. Pellicer-Porres, A. Segura, and D. Kim, *Semicond. Sci. Technol.* **24**, 015002 (2009).
- ⁶⁵M. Nolan, *Thin Solid Films* **516**, 8130 (2008).
- ⁶⁶L. Shi, Z. Fang, and J. Li, *J. Appl. Phys.* **104**, 073527 (2008).
- ⁶⁷D. J. Aston, D. J. Payne, A. J. H. Green, R. G. Egdell, D. S. L. Law, J. Guo, P. A. Glans, T. Learmonth, and K. E. Smith, *Phys. Rev. B* **72**, 195115 (2005).
- ⁶⁸A. Buljan, P. Alemany, and E. Ruiz, *J. Phys. Chem. B* **103**, 8060 (1999).
- ⁶⁹F. Bruneval, Ph.D. thesis, Ecole Polytechnique, 2005.
- ⁷⁰S. Lany and A. Zunger, *Phys. Rev. B* **78**, 235104 (2008).
- ⁷¹R. Shaltaf, G. M. Rignanese, X. Gonze, F. Giustino, and A. Pasquarello, *Phys. Rev. Lett.* **100**, 186401 (2008).
- ⁷²J. Paier, M. Marsman, K. Hummer, G. Kresse, I. C. Gerber, and J. G. Ángyán, *J. Chem. Phys.* **124**, 154709 (2006).
- ⁷³F. Bechstedt, K. Seino, P. H. Hahn, and W. G. Schmidt, *Phys. Rev. B* **72**, 245114 (2005).
- ⁷⁴M. Snure and A. Tiwari, *Appl. Phys. Lett.* **91**, 092123 (2007).
- ⁷⁵D. Scanlon, A. Walsh, and G. Watson, *Chem. Mater.* **21**, 4568 (2009).